Nonreciprocal transmission of microwaves through a long Josephson junction

A. L. Pankratov,[1,2,3] K. G. Fedorov,[4,5,6] M. Salerno,[7] S. V. Shitov,[5,8] and A. V. Ustinov[4,5]

[1]*Institute for Physics of Microstructures, RAS, Nizhny Novgorod, 603950, Russia*
[2]*Center of Cryogenic Nanoelectronics, Nizhny Novgorod State Technical University n.a. R.E. Alekseev, 603950 Nizhny Novgorod, Russia*
[3]*IITMM, Lobachevsky State University of Nizhni Novgorod, 603950 Nizhny Novgorod, Russia*
[4]*Physikalisches Institut, Karlsruhe Institute of Technology, D-76128 Karlsruhe, Germany*
[5]*National University of Science and Technology MISIS, Leninsky prospekt 4, Moscow 119049, Russia*
[6]*Walther-Meißer-Institut, Bayerische Akademie der Wissenschaften, D-85748 Garching, Germany*
[7]*Dipartimento di Fisica "E. R. Caianiello," CNISM and INFM Gruppo Collegato di Salerno, Universitá di Salerno, Italy*
[8]*Kotelnikov Institute of Radio Engineering and Electronics, RAS, Moscow 125009, Russia*

(Received 3 December 2014; published 1 September 2015)

Nonreciprocal microwave transmission through a long Josephson junction in the flux-flow regime is studied analytically and numerically within the framework of the perturbed sine-Gordon model. We demonstrate that the maximum attenuation of the transmitted microwave power occurs when the direction of the flux flow is opposite the direction of the microwave propagation. This attenuation is nonreciprocal with respect to the flux-flow direction and can be enhanced by increasing the system length and proper impedance matching of the junction ends to the external transmission line.

DOI: 10.1103/PhysRevB.92.104501 PACS number(s): 74.50.+r, 03.75.Lm

I. INTRODUCTION

Isolators and circulators transmit microwave power in one direction and do not transmit in the opposite direction. They are used to protect various microwave devices from the harmful effects of standing waves and also to guard amplifiers from unwanted signal reflections. These useful functions become possible due to the nonreciprocal properties of isolators and circulators, which are gained at the price of using rather bulky magnetic materials such as ferrites.

Recently, a demanding application niche for compact cryogenic microwave isolators has been created by the advances in superconducting qubits and rapid progress in circuit quantum electrodynamics [1,2]. Superconducting quantum circuits are operated at millikelvin temperatures and are measured using weak microwave signals, which need to be amplified by low-noise cryogenic amplifiers. Here bulky conventional isolators and circulators become rather inconvenient and, moreover, harmful for superconducting circuits due to their relatively large stray magnetic fields. In this area, there is a great need for compact, preferably on-chip, nonreciprocal microwave devices. A possible way towards implementing such a device is based on parametric modulation [3]. An alternative approach for implementation of the nonreciprocal functionality can employ active transmission line sections with gain in one direction and attenuation in the other. Using a superconducting on-chip flux-flow amplifier [4,5] based on a long Josephson junction (LJJ) provides an opportunity along this path. Such amplifiers are expected to have a wide frequency band [6] and a rather low level of noise [7].

Our recent experiments have revealed the presence of a notable nonreciprocity in transmission of a coherent microwave signal through an LJJ biased in the flux-flow regime [8]. This nonreciprocal behavior can be intuitively explained by interaction of the microwave signal with a moving chain of Josephson fluxons inside the junction. Here microwave signal frequency f_{MW} is typically much lower than the frequency f_{FF} of flux-flow-type Josephson oscillations. A preferred nonreciprocal configuration for propagation of the electromagnetic wave is created by choosing a specific direction of the flux flow given by a combination of polarities of the applied bias current and the in-plane magnetic field. The microwave transmission from one end of LJJ to the other is enhanced when the wave vector of the applied microwave coincides with the direction of the flux flow. In contrast to this, the propagation is damped when the microwave signal is applied to a fluxon's output port of the LJJ. Thus, the LJJ acts as an on-chip isolator for external microwave signals, with its transmission properties being fully controlled by a bias current and an in-plane magnetic field (generated via an on-chip control line). The discussed isolation functionality is somewhat close to the working principle of traveling-wave isolators proposed for optical applications [9,10]. Previous experiments have shown [11,12] that the emission of Josephson radiation from LJJ in the flux-flow regime (at the frequency of flux flow f_{FF}) is negligible from the side where the fluxons enter LJJ (an input port). For this reason, an unwanted emission of such a LJJ isolator back into the incoming microwave line can be neglected.

The above-described operation principle offers an opportunity to create an isolator for microwave cryogenic applications. However, to fulfill the task of constructing a practically useful isolator, one needs to achieve an isolation level comparable to the standard 20–25 dB or better. This benchmark remained beyond reach in the first experiment [8]. To achieve the isolation level needed for useful applications, a better understanding of the physics of the up- and down-conversion processes of microwaves inside the LJJ is required. As the typical impedance of a LJJ is much lower than that of external circuits, one also has to study the impedance-matching conditions of LJJs to an external network.

This paper presents a systematic numerical and analytical study of nonreciprocal microwave transmission through the LJJ in the flux-flow regime. We study nonreciprocal microwave

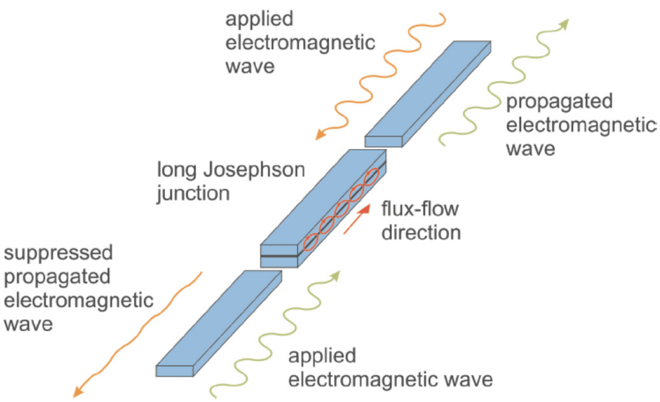

FIG. 1. (Color online) Sketch of a long Josephson junction, subjected to an external microwave signal, studied in Ref. [8].

transmission through the LJJ for different system parameters and impedance-matching conditions.

II. STATEMENT OF THE PROBLEM AND INVESTIGATION OF THE UNMATCHED CASE

In Ref. [8] the nonreciprocal transmission of microwaves in long-overlap Josephson junction (as depicted in Fig. 1) has been studied. A qualitative understanding of the nonreciprocal effect can be gained from the analysis of the perturbed sine-Gordon equation (PSGE)

$$\phi_{tt} + \alpha\phi_t - \phi_{xx} = \beta\phi_{xxt} + \eta - \sin(\phi), \tag{1}$$

with the boundary conditions

$$\phi_x(0,t) = \Gamma + A\sin\Omega t, \;\; \phi_x(L,t) = \Gamma, \tag{2}$$

as an adequate model of a LJJ operating in the flux-flow regime [13]. Here space and time are normalized to the Josephson penetration length λ_J and to the inverse plasma frequency ω_p^{-1}, respectively. Indices t and x denote temporal and spatial derivatives, and ϕ is the Josephson phase difference. Other parameters are normalized as follows: $\alpha = \omega_p/\omega_c$ is the damping, $\omega_p = \sqrt{2eI_c/\hbar C}$, $\omega_c = 2eI_cR_N/\hbar$, I_c is the critical current, C is the LJJ capacitance, R_N is the normal-state resistance, L is the dimensionless length of the junction in units of the Josephson length λ_J, β is the surface loss parameter, and η is the dc bias current density, normalized to the critical current density J_c (here e is the electron charge, and $\hbar$ is the modified Planck constant). Typical parameters of the long Josephson Nb/AlO$_x$/Nb junctions are (see Refs. [8,13]) lengths from a few λ_J to $100\lambda_J$ (note that in [8] $L \approx 18$), $\alpha = 0.1/0.01$, $\beta = 0.1/0.01$.

In the boundary conditions given by Eq. (2), Γ denotes a dc in-plane magnetic field at the edges of the junction normalized to $\lambda_J J_c$, while the ac term, with normalized amplitude A and frequency $\Omega = 2\pi f_{\mathrm{MW}}/\omega_p$ applied at the $x = 0$ boundary, accounts for a microwave radiation applied to the junction. It is well known that the flux-flow regime is achieved when $\Gamma > 2$ and is characterized by an average of $N = \Gamma L/2\pi$ fluxons moving in the direction fixed by the signs of Γ and η on a uniform rotating background $\phi_0 = \omega t + \Gamma x$, where $\omega = V$ is the Josephson oscillation frequency, normalized to ω_p and at the same time the dimensionless voltage. The nonreciprocal effect must be related to a different dynamical behavior of the radiation generated at the $x = 0$ boundary when traveling inside the junction along the flux-flow direction or against it, thus depending on the sign of Γ. In this respect, it is convenient to separate the flux-flow background ϕ_0 from the rest of the field and derive an effective field equation fulfilling the reflective boundary conditions. Note that the linear increase in space of the background ϕ_0 allows satisfying the dc part of the boundary conditions (2). In this approximation one also reproduces the resistive branch $\eta = \alpha\omega$ of the I-V characteristic of the Josephson junction. To account for the ac part of the boundary condition we adopt the approach of Ref. [14] and assume the following ansatz solution:

$$\phi(x,t) = \phi_0 + f_+(x)\cos\Omega t + f_-(x)\sin\Omega t + \psi(x,t) + \theta, \tag{3}$$

where $f_\pm$ are space-dependent functions which have to satisfy the ac part of the boundary condition (2), θ is an arbitrary initial phase, and $\psi(x,t)$ represents the radiation field inside the junction. To simplify the analysis we neglect the surfaces losses in the PSGE, so we put $\beta = 0$ in Eq. (1). It can be readily checked that by substituting Eq. (3) into Eq. (1) one obtains

$$\psi_{xx} - \psi_{tt} - \alpha\psi_t = \alpha\omega - \eta + \sin[\phi_0 + f_+\cos\Omega t + f_-\sin\Omega t + \psi + \theta], \tag{4}$$

with ψ satisfying the reflective boundary conditions

$$\psi_x(0,t) = \psi_x(L,t) = 0, \tag{5}$$

provided that functions $f_\pm(x)$ satisfy

$$\begin{aligned} f_\pm'' + \Omega^2 f_\pm &= \pm\alpha\Omega f_\mp, \\ f_-'(0) = A, \quad f_+'(0) &= f_\pm'(L) = 0. \end{aligned} \tag{6}$$

The system in (6) can be exactly solved (see also [14]), with the explicit expressions for functions $f_\pm$ being

$$f_\pm(x) = \mp\frac{A}{\Omega\sqrt{\alpha^2+\Omega^2}}\frac{h^\pm(x_+,x_-) + h^\pm(x_-,x_+)}{\cos(2L\Omega^+) - \cosh(2L\Omega^-)}, \tag{7}$$

with $\Omega_\pm = [\frac{\Omega}{2}(\sqrt{\alpha^2+\Omega^2} \pm \Omega)]^{\frac{1}{2}}$, $x_\pm = L \pm (x - L)$, and

$$h^\pm(x,y) = \Omega_\pm\cos\Omega_+ y\sinh\Omega_- x \pm \Omega_\mp\cosh\Omega_- x\sin\Omega_+ y. \tag{8}$$

Assuming the field ψ is small, Eq. (4) can be linearized as

$$\begin{aligned} &\psi_{xx} - \psi_{tt} - \alpha\psi_t \\ &= \alpha\omega - \eta + \sum_{m=-\infty}^{+\infty} J_m(f(x))\sin[\tilde{\omega}_m + \Gamma x + m\Phi(x) + \theta] \\ &\quad + \sum_{m=-\infty}^{+\infty} \psi J_m(f(x))\cos[\tilde{\omega}_m + \Gamma x + m\Phi(x) + \theta], \end{aligned} \tag{9}$$

where we have introduced the functions

$$f(x) = \sqrt{f_+(x)^2 + f_-(x)^2}, \;\; \Phi(x) = \tan^{-1}\frac{f_+(x)}{f_-(x)}, \tag{10}$$

and denoted with $J_m(\beta)$ the Bessel function of order m and $\tilde{\omega}_m = \omega + m\Omega$. A solution of Eq. (9) satisfying the boundary condition (5) can be obtained as a Fourier series in the form

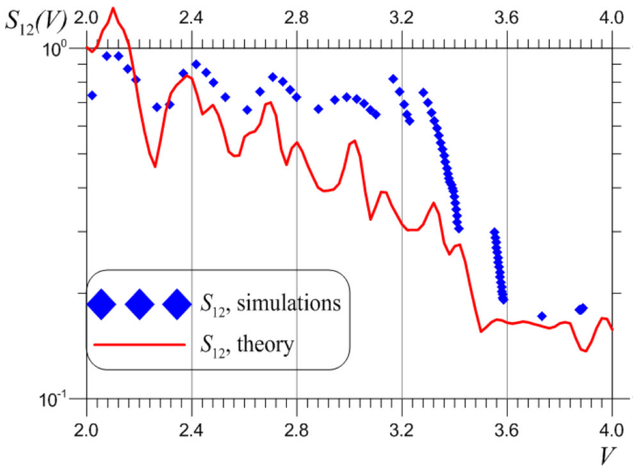

FIG. 2. (Color online) Dimensionless transmitted power S_{12} vs dimensionless voltage for $\alpha = 0.1$, $L = 20$, $\Gamma = 4$, $\omega = 0.231$, and $A = 0.5$ (the external microwave signal propagates against the flux-flow movement).

(see also [14])

$$\psi(x,t) = \sum_n \sum_m [B^+_{nm} c^+_m(t) + B^-_{nm} c^-_m(t)] \cos k_n x, \qquad (11)$$

with coefficients $B^\pm_{nm}$ of the expansion given by

$$B^\pm_{nm} = \frac{(\omega_m^2 - k_n^2) I^\mp_{nm} \pm \alpha \omega_m I^\pm_{nm}}{(\omega_m^2 - k_n^2)^2 + \alpha^2 \omega_m^2},$$
$$I^\pm_{nm} = \frac{1}{L} \int_0^L \cos(k_n x) J_m(f(x)) s^\pm_m(x) dx, \qquad (12)$$

where $c^+_m(t) = \cos(\omega_m t + \theta)$, $c^-_m(t) = \sin(\omega_m t + \theta)$, $s^+_m(x) = \cos[\Gamma x + m\Phi(x)]$, $s^-_m(x) = \sin[\Gamma x + m\Phi(x)]$, and we denoted $k_n = n\pi/L$.

From Eq. (11) one can obtain the amplitudes of phase oscillations at the edges of the junction to estimate the transmission amplitude. While this expression is too complicated to manipulate analytically, it can be evaluated numerically by truncating the series. Let us consider standard S characteristics normalized to the power of the input drive A^2. Here S_{12} corresponds to the transmission of the microwave signal (supplied from the left end, against the flux flow), and S_{21} corresponds to the reversed signal transmission (supplied from the right end, along the flux flow). In Fig. 2 we compare the transmitted power S_{12} computed from the amplitude of the radiation signal (3) and (11) with the one obtained from the numerical simulations. Although the theory slightly overestimates the phenomenon in the main working range, there is clear evidence of the existence of the nonreciprocal effect with a good qualitative agreement between analytical and numerical results. Our analysis is based on the first-order perturbation theory of the sine-Gordon system. For the fluxon dynamics this is usually good enough to get a reasonable quantitative agreement [15]. The nonreciprocity phenomenon, however, involves the propagation of the microwaves on the flux-flow dynamics for which it could be necessary to include also radiative-radiative corrections, which are typically of second order. Indeed, at first order we get the interaction of the radiation injected from the boundary with the fluxons, but at second order we also get the interaction of the injected radiation with the intrinsic radiation generated by the fluxon dynamics. This may explain why the agreement in Fig. 2 is only qualitative.

III. INVESTIGATION OF THE EFFECT OF MATCHING

To associate our results with the experimental data it is interesting to consider a more realistic situation in which the surface losses and boundary loads are included in the model. In this case, however, an analytical treatment is out of reach, and we shall resort to the direct numerical simulations of the PSGE with boundary conditions

$$\phi(0,t)_x + r_L c_L \phi(0,t)_{xt} - c_L \phi(0,t)_{tt} + \beta r_L c_L \phi(0,t)_{xtt} + \beta \phi(0,t)_{xt} = \Gamma - \Delta\Gamma + \Gamma_{12}(t), \qquad (13)$$

$$\phi(L,t)_x + r_R c_R \phi(L,t)_{xt} + c_R \phi(L,t)_{tt} + \beta r_R c_R \phi(L,t)_{xtt} + \beta \phi(L,t)_{xt} = \Gamma + \Delta\Gamma + \Gamma_{21}(t), \qquad (14)$$

which are appropriate for RC loads [13,16]. Here $\Delta\Gamma$ is a small magnetic field difference, and $\Gamma_{12}(t) = A \sin(\Omega t)$ and $\Gamma_{21}(t) = A \sin(\Omega t)$ are ac magnetic fields which are supplied either from the left (Γ_{12}) or from the right (Γ_{21}) junction ends, respectively, but not from the both ends simultaneously. The dimensionless resistances and capacitances, $r_{L,R}$ (normalized on the characteristic impedance of the junction Z_0) and $c_{L,R}$ (normalized to the capacitance $C_0 = 1/\omega_p Z_0$), are the LJJ RC loads placed at the left (output) and at the right (input) ends, respectively [16].

We are going to investigate the nonreciprocal microwave transmission by the direct simulation of Eq. (1) with the boundary conditions (13). Results are compared with both our simplified analytical study (in the corresponding range of validity; see Fig. 2) and with the experiment performed using a device fabricated in a standard Nb-AlO_x-Nb technology [8].

The settings used in our numerical study are the following. The junction length varies from $L = 20$ to $L = 80$, the damping is $\alpha = 0.03$, and the surface losses are $\beta = 0.03$. The signs of the bias current and the magnetic field are chosen such that the fluxons are moving from right to left and the radiation is emitted from the left end of the junction. To supply the maximum ac power to the LJJ, it should be well matched to the external transmission line, so the values of r_L and r_R must vary from 0.5 to 2. In reality, it is difficult to achieve a proper matching due to technical limitations of fabrication processes, so to investigate the physics of the considered effect we will vary r_L and r_R in a broad range. Let us start from the poorly matched case $r_L = r_R = 20$ and the short junction length $L = 20$. The ac signal frequency is fixed at $\Omega = 0.1$ close to experimental values, while its amplitude is set at $A = 0.5$ in most cases except in Fig. 5(a), where dependence on the driving amplitude is studied.

The current-voltage characteristics for $L = 20$, $r_L = r_R = 20$, $c_L = c_R = 10$, and different values of magnetic field Γ

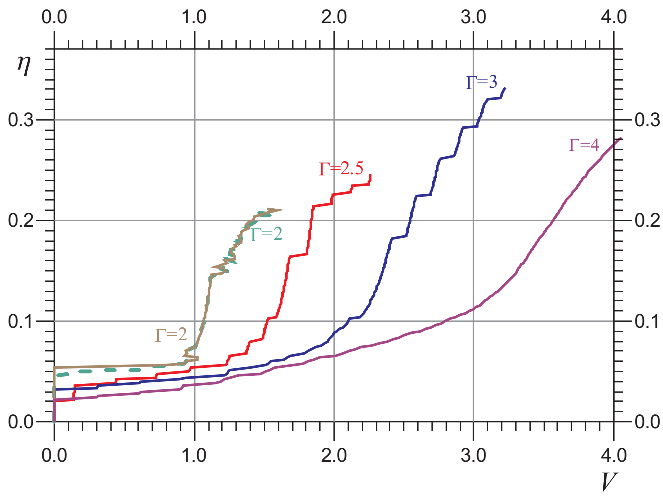

FIG. 3. (Color online) Dimensionless current-voltage characteristic of a LJJ for the mismatched case, $r_L = r_R = 20$, $c_L = c_R = 10$, and $L = 20$.

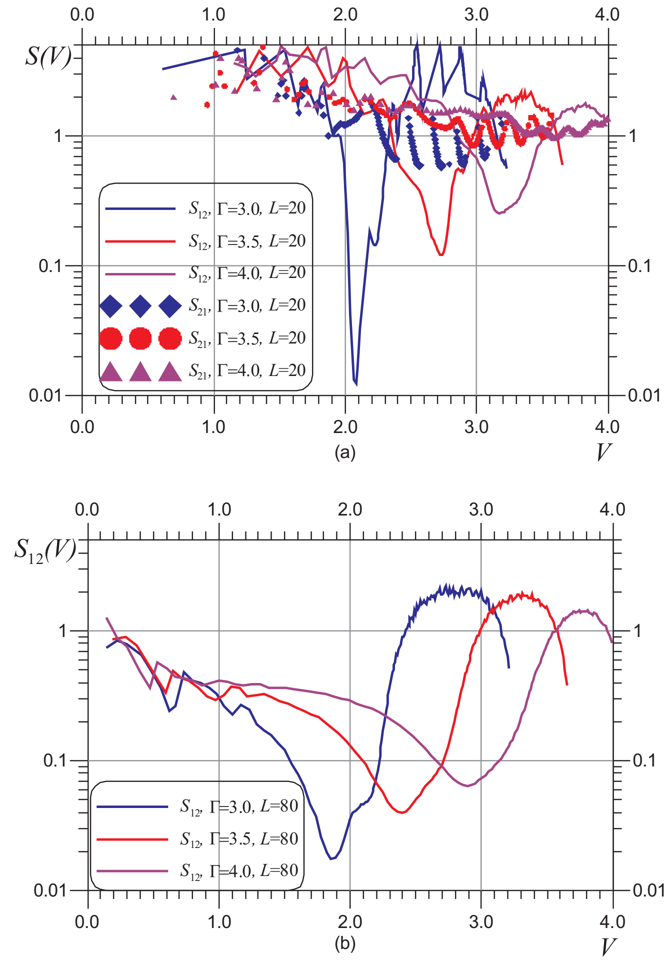

FIG. 4. (Color online) (a) The dimensionless transmitted power S_{12} and S_{21} vs dimensionless voltage for $\alpha = 0.03$ and $\Gamma = 3.0$, $\Gamma = 3.5$, $\Gamma = 4.0$; $r_L = r_R = 20$, $c_L = c_R = 10$. (b) The dimensionless transmitted power S_{12} vs dimensionless voltage for $\alpha = 0.03$ and $\Gamma = 3.0$, $\Gamma = 3.5$, $\Gamma = 4.0$; $r_L = r_R = 20$, $c_L = c_R = 10$, $L = 80$.

(see Fig. 3) look similar to usual experimental curves: one can see the displaced linear slope at $\Gamma = 2.0$ and the Fiske steps at $\Gamma = 2.5$ and $\Gamma = 3.0$, which are smoothed due to surface losses at larger magnetic fields $\Gamma = 4.0$ (the flux-flow steps). All these curves are calculated for the case where ac driving is supplied at the left (output) LJJ end, while the dashed curve is for $\Gamma = 2.0$ and the ac driving supplied from the right (input) junction end. Curves for the higher magnetic fields and the ac driving from the right end are not shown since they nearly coincide with the shown I-V characteristics for the same magnetic fields because the relatively weak ac signal does not affect the I-V characteristics.

Analyzing coefficients of microwave power transmission through the junction S coefficients, one can see from Fig. 4(a) that in the case of small magnetic field Γ (soft vortex chain), the nonreciprocal effect is rather large, and the S_{12} parameter can be around two orders of magnitude. For large magnetic field $\Gamma = 4$ the S_{12} parameter decreases roughly by 50% and becomes comparable to the measured experimental values [8] reported for similar range of parameters. From our numerical studies we also obtain clear indications of how the nonreciprocal effect could be enhanced by properly choosing the parameters. In this respect, we have first investigated the dependence on the junction length L, keeping all other parameters the same. Considering the behavior of the S_{21} parameter [symbols in Fig. 4(a)], one can see that at large magnetic fields the curves slightly oscillate around unity. Note that the I-V curves for $L = 80$ for various values of magnetic field $\Gamma = 2.0$, $\Gamma = 2.5$, $\Gamma = 3.0$ reach larger values of current than in Fig. 3 for $L = 20$. From Fig. 4(b) one can see that the ac signal attenuation for larger lengths in the area of large magnetic field Γ becomes stronger, while for smaller Γ the area of minimal S_{12} increases. For the particular value of the in-plane magnetic field $\Gamma = 4$, we consider the dependence of the effect on the ac signal amplitude [see Fig. 5(a)]. One can observe the paradoxical behavior of S_{12}: the nonreciprocal effect becomes stronger with an increase in the driving amplitude. However, the analysis of the power spectral density for various values of the amplitude clarifies the situation. With an increase in the ac input driving amplitude, the signal amplitude at the opposite end at the basic frequency Ω becomes almost constant up to $A = 5$; however, due to the nonlinearity of the Josephson junction the amplitudes of higher harmonics (at Ω, 2Ω, 3Ω) increase. When calculating S_{12}, only the amplitude at frequency Ω is taken into account, which leads to S_{12} decreasing. It should be noted that for the considered parameters and the amplitudes above $A = 5$, the nonreciprocal effect decreases (the minimum value of S_{12} grows). The nonreciprocal effect can be further improved by a better impedance matching of the LJJ with an external waveguide system. In Fig. 5(b) several curves of S_{12} for the various values of load resistance $r = r_L = r_R$ and capacitance $c = c_L = c_R$ are presented. Here the power of the propagated ac signal can be suppressed by almost up to three orders of magnitude even for large magnetic fields $\Gamma = 4$, so the isolation can be greatly improved. As one can see, the chosen value of the load capacitance $c_L = c_R = 10$ is not the optimal one since stronger attenuation of the transmitted signal is observed at smaller values of the load capacitance. This means

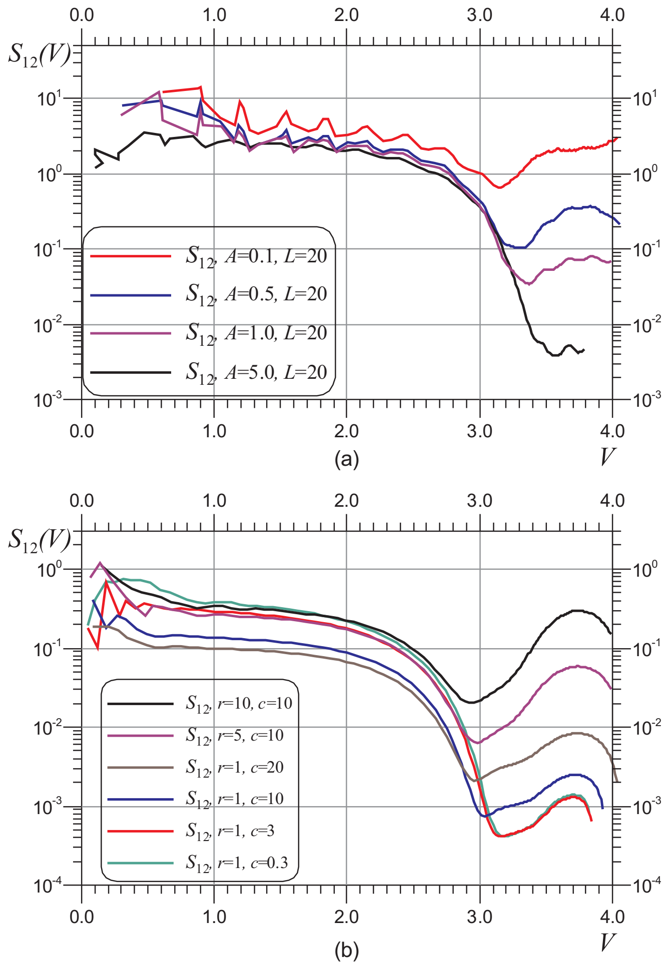

FIG. 5. (Color online) (a) The dimensionless transmitted power S_{12} vs dimensionless voltage for $\alpha = 0.03$, $L = 20$, $\Gamma = 4$, $r_L = r_R = 10$, and $c_L = c_R = 10$ for various values of driving amplitude. (b) The dimensionless transmitted power S_{12} vs dimensionless voltage for $\alpha = 0.03$, $L = 80$, $A = 0.5$, and $\Gamma = 4$ for various values of load resistance $r = r_L = r_R$ and capacitance $c = c_L = c_R$.

that the matching of the structure must be performed in the range of the transmitted signal frequency, while the good matching in the range of flux-flow generation of LJJ is not required.

Figure 6 compares the numerical data (dashed curves) with the experimentally measured transmitted power S_{12} and S_{21} taken from Ref. [8] (solid curves). There is a qualitative agreement between the S parameters. From our study we expect that by increasing the junction length L and by improving the matching at the frequencies of the propagating signal, one should be able to improve the ac signal isolation up to 20–30 dB in future experiments.

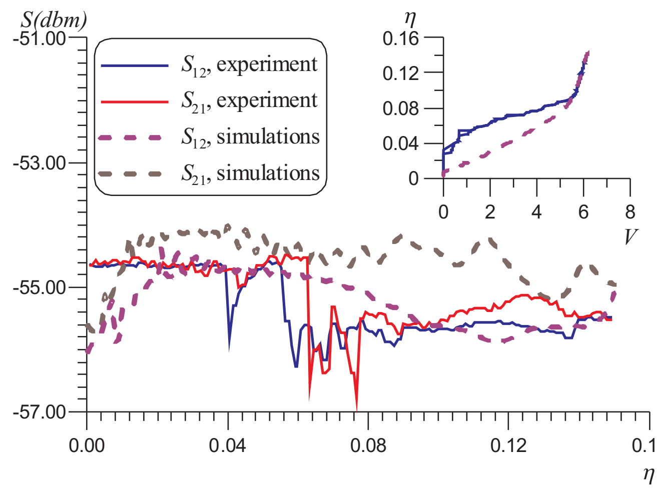

FIG. 6. (Color online) The experimentally measured dimensionless transmitted power S_{12} and S_{21} (solid curves) vs dimensionless current density compared to the numerically simulated data (dashed curves) for $L = 18$, $\alpha = 0.014$, $\Gamma = 7.3$, $r_L = r_R = 10$, $c_L = c_R = 10$, $\beta = 0.007$, $\Delta\Gamma = 0.2\Gamma$, $\omega = 0.231$, and $A = 0.5$. The inset shows a comparison of the dimensionalized current-voltage curves for the same parameters.

IV. CONCLUSIONS

In conclusion, we have investigated, both analytically and numerically, the nonreciprocal microwave transmission through a long Josephson junction in the flux-flow regime within the framework of the sine-Gordon equation. It is demonstrated that the maximum attenuation of the transmitted power occurs when the direction of the fluxon motion is opposite the direction of a microwave propagation. This attenuation is nonreciprocal in respect to the flux-flow direction and can be enhanced by increasing the length of the LJJ and by properly impedance matching it to the external microwave network.

ACKNOWLEDGMENTS

This work was supported by the Ministry for Education and Science of the Russian Federation under Contracts No. 11.G34.31.0062 and No. 3.2054.2014/K and RFBR Grant No. 15-02-05869 and in the framework of the Increase Competitiveness Program of the National University of Science and Technology (MISiS) under Contract No. K2-2014-025 and of Lobachevsky NNSU under Contract No. 02.B.49.21.0003. M.S. acknowledges partial support from the Ministero dell'Istruzione, dell'Università e della Ricerca (MIUR), through a Programmi di Ricerca Scientifica di Rilevante Interesse Nazionale (PRIN) 2010-2011 Grant No. 2010HXAW77-005.

[1] J. Clarke and F. K. Wilhelm, Nature (London) **453**, 1031 (2008).
[2] R. J. Schoelkopf and S. M. Girvin, Nature (London) **451**, 664 (2008).
[3] A. Kamal, J. Clarke, and M. H. Devoret, Nat. Phys. **7**, 311 (2011).
[4] T. Nagatsuma, K. Enpuku, H. Iwakura, and K. Yoshida, Jpn. J. Appl. Phys. **24**, L599 (1985).

[5] J. E. Nordman, Supercond. Sci. Technol. **8**, 681 (1995).
[6] M. A. Ketkar, J. B. Beyer, and J. E. Nordman, IEEE Trans. Appl. Supercond. **9**, 3949 (1999).
[7] C. Granata, A. Vettoliere, and R. Monaco, Supercond. Sci. Technol. **27**, 095003 (2014).
[8] K. G. Fedorov, S. V. Shitov, H. Rotzinger, and A. V. Ustinov, Phys. Rev. B **85**, 184512 (2012).
[9] S. Bhandare, S. K. Ibrahim, D. Sandel, H. Zhang, F. Wuest, and R. Noe, IEEE J. Sel. Top. Quantum Electron. **11**, 417 (2005).
[10] M. S. Kang, A. Butsch, and P. St. J. Russel, Nat. Photonics **5**, 549 (2011).
[11] V. P. Koshelets, S. V. Shitov, L. V. Filippenko, A. M. Baryshev, H. Golstein, T. de Graauw, W. Luinge, H. Schaeffer, and H. van de Stadt, Appl. Phys. Lett. **68**, 1273 (1996).
[12] V. P. Koshelets and S. V. Shitov, Supercond. Sci. Technol. **13**, R53 (2000).
[13] A. L. Pankratov, A. S. Sobolev, V. P. Koshelets, and J. Mygind, Phys. Rev. B **75**, 184516 (2007).
[14] M. Salerno and M. R. Samuelsen, Phys. Rev. B **61**, 99 (2000).
[15] M. Cirillo, N. Gronbech-Jensen, M. R. Samuelsen, M. Salerno, and G. V. Rinati, Phys. Rev. B **58**, 12377 (1998).
[16] C. Soriano, G. Costabile, and R. D. Parmentier, Supercond. Sci. Technol. **9**, 578 (1996).